Neurochemistry International 129 (2019) 104499

Contents lists available at ScienceDirect

Neurochemistry International

journal homepage: www.elsevier.com/locate/neuint

Role of NF-κB in cytochrome P450 epoxygenases down-regulation during an inflammatory process in astrocytes

Cynthia Navarro-Mabarak[a], Irma Beatriz Mitre-Aguilar[b], Rafael Camacho-Carranza[a,c], Clorinda Arias[a], Alejandro Zentella-Dehesa[a,b], Jesús Javier Espinosa-Aguirre[a,*]

[a] Departamento de Medicina Genómica y Toxicología Ambiental, Instituto de Investigaciones Biomédicas, Universidad Nacional Autónoma de México, Ciudad de México, Mexico

[b] Unidad de Bioquímica, Instituto Nacional de Ciencias Médicas y Nutrición Salvador Zubirán (INCMNSZ), Av. Vasco de Quiroga Nº 15, Colonia Belisario Domínguez Sección XVI, Delegación Tlalpan, CP.14080, Ciudad de México, Mexico

[c] Facultad de Ciencias, Universidad Nacional Autónoma de México, Ciudad de México, Mexico

ARTICLE INFO

Keywords:
Cytochrome P450
NF-κB
Epoxygenase
Inflammation
Astrocytes

ABSTRACT

Cytochrome P450 (CYP) epoxygenases and their metabolic products, epoxyeicosatrienoic acids (EETs), have been proposed as important therapeutic targets in the brain. However, CYP expression can be modified by the presence of diverse pro-inflammatory cytokines and the subsequent activation of the NF-κB pathway. It has been indicated that CYP epoxygenases are down-regulated by inflammation in the heart, kidney and liver. However, up to this point, there has been no evidence regarding regulation of CYP epoxygenases during inflammation in the brain. Therefore, in order to explore the effects of inflammation and NF-κB activation in CYP2J3 and CYP2C11 regulation, rat primary astrocytes cultures were treated with LPS with and without IMD-0354 (selective NF-κB inhibitor). *Cyp2j3* and *Cyp2c1*1 mRNA expression was determined by qRT-PCR; protein expression was determined by immunofluorescence and by Western Blot and total epoxygenase activity was determined by the quantification of EETs by ELISA. NF-κB binding sites in *Cyp2j3* and *Cyp2c11* promoter regions were bioinformatically predicted and Electrophoretic Mobility Shift Assays (EMSA) were performed to determine if each hypothetic response element was able to bind NF-κB complexes. Results shown that LPS treatment is able to down-regulate astrocyte CYP2J3 and CYP2C11 mRNA, protein and activity. Additionally, we have identified NK-κB as the transcription factor involved in this regulation.

1. Introduction

Cytochrome P450 (CYP) is a group of related enzymes highly conserved in nature. In humans, 57 CYP genes have been found, and research on the endogenous role of these enzymes continues. CYP enzymes metabolize approximately 75% of known drugs and promote their elimination from the body. However, CYP enzymes can metabolize a wide variety of endogenous substrates (cholesterol, hormones, fatty acids) (Dutheil et al. 2008) and they are involved in several important metabolic pathways, even in the brain, where they have been proposed as a therapeutic target for neurodegenerative diseases (Navarro-Mabarak et al. 2018).

CYP epoxygenases mediate the oxidation of the arachidonic acid (AA) to epoxyeicosatrienoic acids (EETs). The CYP2C and 2J subfamilies are the CYP enzymes with the highest epoxygenase activity, although other CYP isoforms, including CYP1A, 2B, and 2E, also mediate epoxidation reactions, albeit to a lesser extent (Capdevila and Falck, 2000). CYP epoxygenases add one oxygen atom to one of the four AA double bonds, resulting in the formation of four regioisomeric acids that are named according to the number corresponding to the carbons involved in the epoxide (5,6-, 8,9-, 11,12-, and 14,15-EET). The EETs can be subsequently hydrolyzed by the soluble epoxide hydrolase enzyme (sEH) into metabolites with lower biological activity, the dihydroxyeicosatrienoic acids (DHETs) (Stables and Gilroy, 2011; Morisseau and Hammock, 2013). In the central nervous system (CNS), the expression of CYP epoxygenases and sEH has been characterized in the brain and its associated vasculature (Carver et al. 2014; Dutheil et al. 2009), as well as in specific cell types such as astrocytes (Liu and Alkayed, 2005; Rawal et al. 2009) and neurons (Ruparel et al. 2012). EETs display diverse biological properties, including cell proliferation,

* Corresponding author. Universidad Nacional Autónoma de México, Departamento de Medicina Genómica y Toxicología Ambiental, Avenida Universidad 3000, Ciudad de México, C.P. 04510, Mexico.

E-mail address: jjea@biomedicas.unam.mx (J.J. Espinosa-Aguirre).

https://doi.org/10.1016/j.neuint.2019.104499
Received 3 April 2019; Received in revised form 9 June 2019; Accepted 1 July 2019
Available online 02 July 2019
0197-0186/

migration, angiogenesis, and vasodilation in vascular endothelial tissue (where they have mostly been studied) (Spector and Norris, 2007). It has also been reported that EETs have potent anti-inflammatory activity, mediated primarily by inhibition of the NF-κB pathway, either through inhibition of IKK (IκB kinase) complex activity or by the activation of nuclear receptors PPAR-α (peroxisome proliferator-activated receptor-α) and PPAR-γ (Fang et al. 2005, 2006; Node et al. 1999). In addition, EETs inhibit the transcription of cyclooxygenase-2 (COX-2), a feature that has been shown to have synergistic anti-inflammatory properties when combined with other known anti-inflammatory agents (Inceoglu et al. 2008; Schmelzer et al. 2006; Liu et al. 2010). In the brain, it has been demonstrated that the EETs can improve the neuroinflammation generated in models that simulate both hemorrhagic and ischemic cerebrovascular events (Koerner et al. 2008; Zhang et al. 2007) or traumatic brain injury (Hung et al., 2017). The sEH inhibition or the CYP epoxygenases overexpression (and the subsequent increase in EETs levels), has demonstrated to be neuroprotective, as it increases cell viability, reduces neuronal apoptosis and enhances neurite outgrowth, synaptic neurotransmission and plasticity (Li et al. 2018; Wang et al. 2018; Wu et al. 2015). Therefore, CYP epoxygenases and sEH have acquired increasing attention as therapeutic targets for neurodegenerative diseases (Navarro-Mabarak et al. 2018), where EETs have demonstrated to counteract many of the etiological characteristics of Parkinson's (Lakkappa et al. 2016, 2018, 2019) and Alzheimer's disease (Sarkar et al. 2014).

However, although EETs are now considered important modulators of inflammation, it has been reported that CYP expression, protein levels, and activity all change with alterations in the levels of pro-inflammatory cytokines (Abdel-Razzak et al. 1993; Nicholson & Renton 2001, 2002; Aitken and Morgan, 2007). It is well known that pro-inflammatory cytokines activate the NF-κB pathway (Baldwin, 1996; Minogue et al. 2012; Schütze et al. 1995), and it has been demonstrated that cytokine-dependent CYP regulation is due to NF-κB activation (Morgan, 2001; Ke et al. 2001; Gu et al. 2006; Iber et al. 2000; Bell and Strobel, 2012). The NF-κB transcription factor can regulate CYP enzymes at different levels by binding directly to response elements in the promoter region of their genes, through mutual repression of some nuclear receptors involved in CYP regulation, and by affecting CYP protein stability (Zordoky and El-Kadi, 2009). Anwar and colleagues have reported that the CYP epoxygenases 2C11 and 2J3 are downregulated in the heart, kidney, and liver during a systemic inflammatory process in rat (Anwar-mohamed et al. 2010). However, the response of CYPs to inflammation depends on the evaluated organ or cell type. For example, CYP2E1 expression and protein levels are decreased in the heart and liver during a systemic inflammatory process (Anwar-mohamed et al. 2010). But, in the brain, CYP2E1 is induced *in vivo* during an inflammatory ischemic injury and *in vitro* by LPS or IL-1β administration to astrocytes (Tindberg et al. 1996; Kelicen and Tindberg, 2004). To date, there is no evidence that demonstrates the regulation of CYP epoxygenases during an inflammatory process in the brain. Therefore, due to the relevance that these enzymes have acquired in the brain, the aim of this work was to determine whether an inflammatory process and the activation of NF-κB pathway is able to modify CYP2J3 and CYP2C11 expression, protein levels and activity in astrocytes.

2. Materials and methods

2.1. Reagents

Eagle's Basal Medium (BME), Glucose, Lipopolysaccharide (LPS) from *Escherichia coli* 0127: B8, IMD-0354 [N-(3,5-bis-trifluoromethyl-phenyl)-5-chloro-2-hydroxy-benzamide], and Poly (2′-deoxyinosinic-2′-deoxycytidylic acid) sodium salt (Poly dI dC) (SIGMA-Aldrich). Glutamine, Penicillin-Streptomycin, and Trypsin inhibitor (Gibco). Fetal Bovine Serum (FBS) (Byproductos). Chicken anti-glial fibrillary acidic protein (GFAP) polyclonal antibody and donkey anti-chicken IgG biotin-SP-conjugated antibody (Merck Millipore). Mouse anti-glyceraldehyde-3-phosphate dehydrogenase (GAPDH) monoclonal antibody (GeneTex). Rat TNF-α ELISA kit (PIERCE). 11,12-EET/DHET ELISA kit and mouse monoclonal anti-CYP2C11 antibody (Detroit R&D). ECL prime Western Blotting detection reagent (General Electric-Amersham). Deoxyribonuclease I (DNAse), Oligo (dT), Ribonuclease inhibitor (RNAse OUT), Moloney murine leukemia virus reverse transcriptase (M-MLV RT) and goat anti-rabbit Alexa Fluor 488 (Invitrogen Life Technologies). TRIzol (Ambion Life Technologies). TaqMan Multiplex Master Mix (Applied Biosystems). NF-κB consensus Gel Shift Oligonucleotide, NF-κB consensus mutated Gel Shift Oligonucleotide, rabbit polyclonal anti-NF-κB p65 and mouse monoclonal anti-CYP2J2 antibodies (Santa Cruz Biotechnology). Texas Red Avidin D (VECTOR Laboratories).

2.2. Primary astrocytes culture

The protocol for the use and handling of all the animals in this study was approved by the local Committee for Animal care (ID: 249) of the Biomedical Research Institute at the National Autonomous University of Mexico. The astrocytes were isolated from the cortex of 2-day-old male Wistar rats obtained from the Animal care unit, as described by Moran and Patel (1989) with some modifications (Moran and Patel, 1989). Each culture was derived from the cells pooled from four rat cortices. In brief, the cortices were isolated and the meninges and blood vessels were removed. The cortices were cut into small pieces and digested in 0.25 mg/ml trypsin at 37 °C for 8 min. Digestion was stopped with 1 mg/ml Trypsin inhibitor in the presence of 0.003% DNase at room temperature. The tissue was dissociated with a pipette and filtered in mesh. After centrifugation, the cells were diluted with fresh medium. Culture medium consisted of BME supplemented with 10% heat-inactivated FBS, 2 mM glutamine, 750 mg glucose, 50 U/ml penicillin and 50 μg/ml streptomycin. Astrocytes were grown in a humidified 37 °C, 5% CO_2 tissue-culture incubator until they reached 90–95% confluency (at approximately 10 days of incubation), state where contact inhibition prevents further cell division (Lange et al. 2012). The culture medium was replaced with fresh medium every third day. To confirm the predominance of astrocytes in the culture, the percentage of GFAP-positive cells was determined by immunofluorescence. We found that astrocytes were > 99% of the cells present in the culture as no microglial cells were found by Iba-1 staining Supplementary Fig. 1).

2.3. Immunofluorescence

Astrocytes were grown on glass coverslips until they reached 90% confluency in 12-well plates. After treatment, the medium was removed and the cells were washed once with cold phosphate-buffered saline (PBS), fixed with 1% paraformaldehyde/0.1 M phosphate buffer (PB) for 10 min at 4 °C, and washed three times with 0.1 M PB/0.3% Triton X-100. The cells were permeabilized with the wash solution for 10 min at room temperature in agitation and then blocked with 0.1 M PB/0.3% Triton X-100/10% FBS for 2 h (at room temperature) or overnight (at 4 °C). Primary antibodies were prepared in the blocking solution (anti GFAP 1:1000; anti Iba-1 1:1000; anti CYP2C11 1:1000; anti CYP2J3 1:500) and the cells were incubated with them overnight at 4 °C in agitation. Then, the coverslips were washed three times with 0.1 M PB/0.3% Triton X-100 and incubated with the corresponding secondary antibody (1:2500). Coverslips were then analyzed with an Olympus Disk-Spinning Unit (DSU) IX2 microscope. Four different experiments were performed (n = 4) and the images were obtained.

2.4. Astrocytes treatment

The culture medium was replaced with fresh medium 18 h before

treatments. Cells were treated with 100 ng/ml LPS (mRNA, protein and EETs determination); 100, 200, 400, and 800 ng/ml LPS (immunofluorescence and protein determination) or 500 ng/ml LPS (EMSAs). The concentrations used of LPS were within the lower range of the concentrations used in previous works (Tindberg et al. 1996; Nicholson and Renton, 1999, 2002; Kelicen and Tindberg, 2004). The NF-κB specific inhibitor IMD-0354 was concurrently added to a final concentration of 1 ng/ml when indicated. It has been demonstrated that IMD-0354 inhibits the phosphorylation of IκB and thus finally inhibits the phosphorylation of NF-κB and its translocation into the nucleus (Onai et al. 2004; Kanduri et al. 2011). Furthermore, NF-κB downstream regulated genes has been proved to be affected by IMD-0354 inhibition, like pro-inflammatory cytokines production (Sugita et al. 2009; Ogawa et al. 2011; Onai et al. 2004).

2.5. TNF-α quantification

TNF-α was determined from the supernatant of cultured astrocytes treated with 100 ng/ml LPS at 6, 12, and 24 h after treatment. The supernatant was recovered and centrifuged to remove any cell fraction. The quantification was performed by ELISA with a commercial kit. The procedure was performed according to the manufacturer's specifications. Concentrations were determined from four different cultures (n = 4). The absorbance was read at 450 nm. The concentrations were calculated from a standard curve.

2.6. RNA isolation and cDNA synthesis

Total RNA was obtained from the culture plates using TRIzol reagent, in accordance with the manufacturer's instructions. The RNA was quantified spectrophotometrically at 260 nm. The purity of the samples was determined by the spectrophotometric ratio A_{260}/A_{280} (ratios > 1.85) and the integrity was confirmed by denaturing electrophoresis of the samples and by observation of them with ethidium bromide. Thereafter, cDNA was obtained from 1 μg of total RNA by reverse transcription using the M-MLV RT, according to the manufacturer's specifications.

2.7. Quantification of mRNA expression by qRT-PCR

Quantitative analysis of CYP mRNA expression was performed by real time-polymerase chain reaction (RT-PCR). Commercial TaqMan gene expression primers (Applied Biosystems) were used to detect *Cyp2j3* (Rn00598500), *Cyp2c11* (Rn01502203), and *GAPDH* (*Rn99999916)*. *GAPDH* was selected as the housekeeping gene because its expression remained constant under our experimental conditions Supplementary Fig. 2). RT-PCR was performed with a Corbett Rotor-Gene 6000 (QIAGEN). For the amplification, the reactions were incubated at 55 °C for 2 min, and then at 95 °C for 10 min, followed by 40 cycles at 95 °C for 15 s plus 1 min at 60 °C. All reactions were performed in triplicate, with the cDNA obtained from four different experiments (n = 4). The expression levels were calculated by ΔΔCT mathematical algorithm, using the Rotor-Gene 6000 Series Software 1.7. The results are shown as the expression levels of *Cyp2j3* and *Cyp2c11* in relation to *GAPDH* ± SD, taking as calibrator the control for each evaluated time.

2.8. Protein immunodetection by Western Blot

After 24 h of LPS and LPS + IMD-0354 treatments, the medium was removed and the cells were washed once (2 ml) and scraped for recovery with PBS 1X. The suspension was centrifuged and the pellet was disintegrated with extraction buffer (50 mM Tris-HCl pH = 7.5, 150 mM NaCl, 1% (v/v) of the NP40 detergent and 0.5% (w/v) of sodium deoxycholate). The homogenate was then sonicated in 3 cycles of 10 s, 3 times, always in ice. The amount of total protein in the sample was quantified by the Bradford method. Sixty micrograms of total protein were separated using 11% SDS-PAGE and were transferred to 0.45 mm nitrocellulose sheets. The nitrocellulose membranes were blocked for 2 h with 5% albumin in 0.3% TBS-Tween at room temperature. Thereafter the membranes were incubated with the corresponding primary antibodies (anti CYP2J2 1:500; anti CYP2C11 1:500; anti GAPDH 1:5000) overnight at 4 °C. The membranes were then washed three times with 0.3% TBS-Tween. The corresponding secondary antibody was incubated for 1 h at room temperature (1:5000) and the membranes were then washed two times with 0.3% TBS-Tween and one time with TBS. The chemiluminescence reaction was performed with ECL prime Western Blotting detection reagent and the resulting images were obtained with a Kodak GEL Logic 1500 imaging system. The relative quantification was carried out determining band intensities with ImageJ software. Protein levels were determined from three independent experiments (n = 3).

2.9. 11,12-EET + 11,12-DHET determination

To determine CYP epoxygenase activity, 11,12-EET and its hydrolyzed product, 11,12-DHET, were measured from the cultured astrocytes using a commercial ELISA kit according to the manufacturer's specifications. Briefly, after 24 h of treatment, the medium was removed and the cells were washed once with PBS/0.1 mM TPP (triphenylphosphine). Cells were scraped, recovered, and sonicated in this buffer. Once sonicated, the homogenates were acidified with acetic acid to a pH of 3–4. Then, three extractions with ethyl acetate were performed on the acid homogenates, thereby recovering the organic phase each time, each of which were stored together. The pooled ethyl acetate extraction was evaporated until it was fully dried up under nitrogen gas, and the dried residue was then dissolved in 20 μl of ethanol. In order to change EETs to DHETs, an acidic hydrolysis was performed by adding 20 μl of acetic acid during 18 h at room temperature. After the reaction, 60 μl of water was added and the samples were extracted three times with equal volume of ethyl acetate. The pooled ethyl acetate extract was evaporated until it was fully dried up under nitrogen gas, and the dried residue was then dissolved in 30 μl of ethanol. To prepare a stock solution, each sample was diluted with 90 μl of TBS 10X to obtain a final volume of 120 μl. To perform the ELISA, each sample was diluted 20X. Total epoxygenase activity from three independent experiments was measured (n = 3).

2.10. Nuclear cell extracts

Nuclear extracts were obtained as originally described (Dignam et al. 1983) with some modifications (López-Bojórquez et al. 2004; Blancas-Flores et al. 2012). After treatment, astrocytes were washed twice with cold PBS, scraped, and centrifuged at 850 × *g* for 5 min to obtain a pellet. The cell pellet was frozen in a dry ice/acetone bath for 3 min. After freezing, the cells were broken by allowing them to thaw in hypotonic buffer (10 mM Hepes, 10 mM KCl, 1.5 mM $MgCl_2$, 1 mM DTT, pH 7.9) for 10 min at 4 °C. Nuclei and cytoplasm were separated by centrifugation at 1,160 × *g*. The nuclear fraction was resuspended in hypertonic buffer (20 mM Hepes, 400 mM NaCl, 1.5 mM $MgCl_2$, 25% v/v glycerol, 0.2 mM EDTA, 1 mM DTT, 0.5 mM PMSF, pH 7.9), and maintained in vortex agitation for 30 min at 4 °C. The suspension was centrifuged at 18,600 × *g* for 20 min at 4 °C. The supernatants were collected and the protein content in them was determined by the Bradford assay. Supernatant aliquots were stored at −70 °C until they were used.

2.11. Database sequence analysis

A search for putative NF-κB binding sites within the *Cyp2j3* and *Cyp2c11* promoter region was conducted. The search was carried out with AliBaba 2.1 free software (BIOBASE) using 4500 base pair upstream of ATG start site.

Table 1
Single stranded sense and antisense oligonucleotides used for EMSA assay.

Identifier	5′ Sense sequence 3′	5′ Antisense sequence 3′
2C11 1	AGTCACAGGGAATTTCCCAGGC	GCCTGGGAAATTCCCTGTGACT
2C11 2	AGTTGAGGGGAGACTCCCAGGC	GCCTGGGAGTCTCCCCTCAACT
2C11 3	AGTTGAGTGGAATCCCTCAGGC	GCCTGAGGGATTCCACTCAACT
2C11 4	AGTTGAGCGGAAATTCCCAGGC	GCCTGGGAATTTCCGCTCAACT
2J3 1	AGTTAGAGGGACTTCCTCAGGC	GCCTGAGGAAGTCCCTCTAACT
2J3 2	AGTTGAGAGAAATTCCCCAGGC	GCCTGGGGAATTTCTCTCAACT
2J3 3	AGTTGAGGGAAATCCAACAGGC	GCCTGTTGGATTTCCCTCAACT
2J3 4	AGTTGAGAGGAGTCTCCCAGGC	GCCTGGGAGACTCCTCTCAACT
Consensus	AGTTGAGGGGACTTTCCCAGGC	Supplied as double-stranded DNA
Consensus mut	AGTTGAGGCGACTTTCCCAGGC	Supplied as double-stranded DNA
sox2	AACTGCACATGGGTGTGTGCAAACCGT (Martínez-Ramírez et al. 2017)	Supplied as double-stranded DNA

2.12. Oligonucleotide labeling with γ^{32}P-ATP

Single stranded oligonucleotides were constructed with 22 bases containing the predicted NF-κB binding sequences (Invitrogen Life Technologies) (Table 1; Fig. 5). Single stranded sense and antisense oligonucleotides were aligned at 65 °C and were kept at room temperature overnight (approx. 16 h). Twenty nanograms (20 ng) of the double stranded oligonucleotides were labeled with γ^{32} P-ATP. The labeling reaction was carried by a T4 polynucleotide kinase (Thermo Scientific) in the presence of the 10x reaction buffer A, incubating at 37 °C for 30 min and stopping the reaction by heating it at 65 °C for 15 min followed by the addition of 30 µl of TBE 1X. The labeled oligonucleotides were stored properly at −70 °C until they were used.

2.13. Electrophoretic mobility shift assay

To perform the Electrophoretic Mobility Shift Assays (EMSAs), 20 µg of the nuclear protein from astrocytes stimulated with 500 ng of LPS for 60 min were incubated with 2 µl (1 ng) of the corresponding γ^{32}-P-labeled oligonucleotide (Table 1). The binding reactions were carried out by incubating on ice for 60 min in the reaction buffer (20 mM HEPES, 50 mM KCl, 20% glycerol, 0.2 mM EDTA, 0.5 mM PMSF, 1 mM DTT, 1 µg/ml BSA, 1 mg/ml poli-dI-dC). The reaction mixture was loaded onto a 6.5% non-denaturing polyacrylamide gel and resolved at 80 V for 1 h and then at 120 V for 50 min. Electrophoresis was carried out in TBE 1X buffer. The gel was dried and the DNA-protein complexes were visualized by exposing the gel to a Storage Phosphor Screen. The screen was read in a Typhoon 9400 *Phosphorimager* and analyzed with ImageQuant software (Molecular Dynamics, San Francisco, CA). NF-κB identity in the DNA-protein complexes was corroborated by supershift assays with a NF-κB anti-p65 antibody. An antibody anti-cIAP1 (cellular Inhibitor of Apoptosis Protein 1), kindly provided by Dr. Alejandro Zentella-Dehesa was used as negative control in the supershift assay. NF-κB consensus commercial oligonucleotide was used as positive binding control. NF-κB consensus mutated commercial oligonucleotide was used as negative binding control. Also competition assays were performed using unlabeled (cold) specific and non-specific oligonucleotides. A putative sox2 binding sequence oligonucleotide (SOX2 (S3)) (Martínez-Ramírez et al. 2017), kindly provided by Dr. Marcela Lizano, was used as negative binding control in the competition assays (Table 1). Four different experiments (n = 4) with the nuclear extracts obtained from four different primary cultures were performed and the images from the EMSAs were obtained to validate reproducibility.

2.14. Statistical analysis

Data were analyzed using ANOVA, and Fisher's LSD procedure was used for multiple comparisons. Homogeneity of variance was analyzed using Levene's test. When heterogeneity of variance was detected, Welch's ANOVA was used. Block design was used when necessary. The differences were considered significant when $p < 0.05$. To perform the statistical analysis, we used SAS 9.0 software.

3. Results

3.1. LPS treatment induced the production of TNF-α. in astrocytes

It has been established that stimulation of astrocytes with LPS leads to the production of pro-inflammatory cytokines (Minogue et al. 2012). To corroborate that 100 ng/ml of LPS lead to an inflammatory response in our model, the production of TNF-α was measured from the control supernatants and stimulated cultures using a specific rat TNF-α ELISA kit. We found that stimulated astrocytes produced approximately 25 times more TNF-α than controls ($p < 0.05$; Table 2), reaching a production of approximately 3 ng/ml, as has been seen in previous reports (Minogue et al. 2012).

3.2. LPS-induced inflammation caused a decrease in Cyp2j3 and Cyp2c11 mRNA expression, and this effect was prevented when NF-κB activity was inhibited

Primary astrocyte cultures were stimulated or not with 100 ng/ml LPS, or 100 ng/ml LPS +1 ng/ml IMD-0354, and CYP epoxygenase mRNA expression was evaluated at different time points. LPS treatment significantly decreased *Cyp2j3* and *Cyp2c11* expression by more than 50% compared to controls at all evaluated time points ($p < 0.05$; Fig. 1). It is worth noting that LPS treatment decreased *Cyp2c11* expression in a time-dependent manner, reaching a decrease of up to 90% at 24 h (Fig. 1B). LPS treatment triggered the production of pro-inflammatory cytokines like TNF-α, which in turn led to the activation of NF-κB pathway (Minogue et al. 2012). To investigate the role of NF-κB in CYP epoxygenases regulation, astrocytes were co-treated with LPS and IMD-0354. *Cyp2j3* down-regulation was almost completely prevented by the addition of IMD-0354, and reached the control levels at 12 h of treatment ($p < 0.05$; Fig. 1A). On the other hand, *Cyp2c11* down-regulation was only partially prevented by NF-κB inhibition at 6 and 12 h, but it could not be prevented at 24 h of treatment ($p < 0.05$; Fig. 1B).

Table 2
TNF-α production by astrocytes after LPS treatment. TNF-α levels were measured from recovered supernatants using a specific rat TNF-α ELISA kit.* ($p < 0.05$).

Treatment	Time of exposition	[TNF-α] Mean (pg/ml)	SD
Control	6 h	90	40
100 ng/ml LPS		**2154***	832
Control	12 h	135	85
100 ng/ml LPS		**3131***	1680
Control	24 h	109	35
100 ng/ml LPS		**3156***	1557

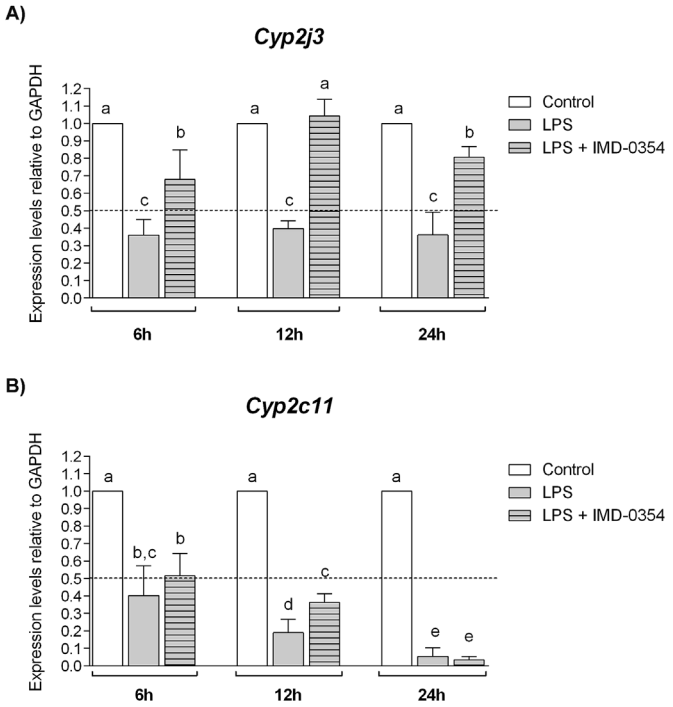

Fig. 1. *Cyp2j3* and *Cyp2c11* relative gene expression levels. Astrocytes primary cultures were stimulated or not with LPS and LPS + IMD-0354 (selective NF-κB inhibitor). *Cyp2j3* (A) and *Cyp2c11* (B) relative expression levels were determined by qRT-PCR. Expression levels are shown relative to *GAPDH* ± SD (n = 4). Data were analyzed for multiple comparisons using ANOVA, and Fisher's LSD procedure. The differences were considered significant when $p < 0.05$. Means with the same letter are not significantly different; means with different letter are significantly different between each other.

3.3. CYP2J3 and CYP2C11 protein levels are down-regulated in a LPS-dose-dependent manner

In order to determine whether LPS-mediated *Cyp2j3* and *Cyp2c11* down-regulation could translate into a decrease in CYP epoxygenase protein levels, astrocytes were treated with increasing concentrations of LPS (from 100 to 800 ng/ml) for 24 h. The CYP protein levels were determined by immunofluorescence and by Western Blot. Immunofluorescence images showed that CYP2J3 and CYP2C11 are localized predominantly around the astrocyte nucleus, in accordance to the characteristic localization of CYPs in the endoplasmic reticulum. It could also be observed that CYP2J3 (Fig. 2A) and CYP2C11 (Fig. 3A) signal decreased in an apparent dose-response manner. However, to confirm quantitatively this effect, CYP protein levels were determined by Western Blot (Figs. 2B and 3B). CYP2J3 and CYP2C11 protein levels were significantly decreased from 100 ng/ml onwards of LPS treatment ($p < 0.05$; Figs. 2C and 3C), but only CYP2C11 followed a significant dose-response effect ($p < 0.05$; Fig. 3C). Also, it was found that CYP2C11 protein levels decreased to a greater extent (reaching a maximum decrease of 78%, with a stimulation of 800 ng of LPS) than CYP2J3 protein levels (reaching a maximum decrease of 50% with a stimulation of 800 ng of LPS). These results are in accordance with the effect of LPS observed in the transcription of *Cyp2j3* and *Cyp2c11*, in which *Cyp2c11* mRNA levels were decreased into a greater extent.

3.4. Inhibition of NF-κB pathway partially prevented CYP2J3 and CYP2C11 protein levels down-regulation

The CYP2J3 and CYP2C11 protein levels were significantly decreased by LPS treatment (100 ng/ml, 24 h), and this effect was partially prevented when 1 ng/ml of IMD-0354 was added concurrently ($p < 0.05$; Fig. 4A and B). These results agree with those obtained at the transcription level, mainly for CYP2J3 (Fig. 4A), given that its transcripts almost reached control levels at 6 and 24 h, and reached control levels at 12 h of IMD-0354 concurrent treatment (Fig. 1A). CYP2C11 protein levels down-regulation was also partially prevented when NF-κB pathway was blocked (Fig. 4B), like its mRNA levels at 6 and 12 h of treatment (Fig. 1B).

3.5. Total epoxygenase activity is decreased after LPS treatment, and this effect was prevented when NF-κB activity was inhibited

NF-κB not only can regulate CYP enzymes at the transcriptional or protein level, but can also interfere ultimately with the activity of the enzyme (Zordoky and El-Kadi, 2009). To investigate whether LPS-induced inflammation could affect total epoxygenase activity, as well as the role of NF-κB in this regulation, astrocytes were treated with 100 ng/ml LPS or LPS +1 ng/ml IMD-0354 for 24 h, and 11,12-EET + 11,12-DHET was measured from the cultured astrocytes. It was chosen to measure both metabolites due to the fast conversion of EETs to DHETs by sEH. The 11,12-EET has been previously identified as the EET with the greatest anti-inflammatory activity (Node et al. 1999); therefore, it was chosen as the representative epoxide to be quantified. Total epoxygenase activity was significantly decreased after LPS treatment, measured as 11,12-EET + 11,12-DHET levels ($p < 0.05$; Fig. 5). The inhibition of NF-κB activity could completely prevent this effect, as EETs reached control levels when IMD-0354 was concurrently added ($p < 0.05$; Fig. 5), demonstrating that LPS-induced inflammation affects EETs production in astrocytes by the activation of NF-κB pathway.

3.6. NF-κB is able to bind specifically, but with different affinities, to all the response elements found in the promoter region of Cyp2j3 and Cyp2c11

Four putative NF-κB binding sites were found within *Cyp2j3* and *Cyp2c11* promoter regions using the AliBaba 2.1 software (Table 1; Fig. 6). EMSAs were performed to determine whether NF-κB complexes were able to recognize and bind to the four putative response elements (Fig. 7). Nuclear proteins from astrocytes stimulated with or without LPS were used to perform the binding reactions. Two major DNA-protein complexes were identified when the binding reactions were performed with the consensus sequence, but only the heaviest complex was increased with LPS treatment. Additonally, only the heaviest complex disappeared when the mutated consensus sequence was used in the binding reactions (Fig. 7). Therefore, the heaviest complex was chosen as the complex of interest. NF-κB was able to bind to the four putative response elements of each of the *Cyp2j3* and *Cyp2c11* genes, but with different affinities. CYP2J3 1, CYP2J3 2, CYP2C11 1 and CYP2C11 4 were the sequences with the greatest binding affinity, observed as a thicker and more intense band (Fig. 7). CYP2C11 1 sequence even showed more affinity than the commercial consensus sequence (Fig. 7B, lane 5). In order to determine the identity of NF-κB in the DNA-protein complexes, supershift assays were performed using 300, 600, or 1200 ng of NF-κB anti-p65 antibody. Only the sequences with the greatest binding affinities were tested in the supershift assays (CYP2J3 1, CYP2J3 2, CYP2C11 1 and CYP2C11 4) (Supplementary Fig. 3). The addition of the anti-p65 antibody resulted in a subtle supershift of the bands and a reduction in the DNA-protein complexes, observed as thinner and less intense bands (Supplementary Fig. 3 and Fig. 8, lane 9), demonstrating the identity of NF-κB. To further demonstrate the identity of NF-κB, an antibody against a protein different from NF-κB (anti-cIAP1) was used as negative control (Fig. 8, lane 10), and it was not observed a supershifted band, neither a reduction in the DNA-protein complex.

Additionally, in order to evaluate whether the putative binding sites were able to compete with the consensus commercial sequence to generate the DNA-protein complexes, 100-fold (100X) of cold CYP2C11

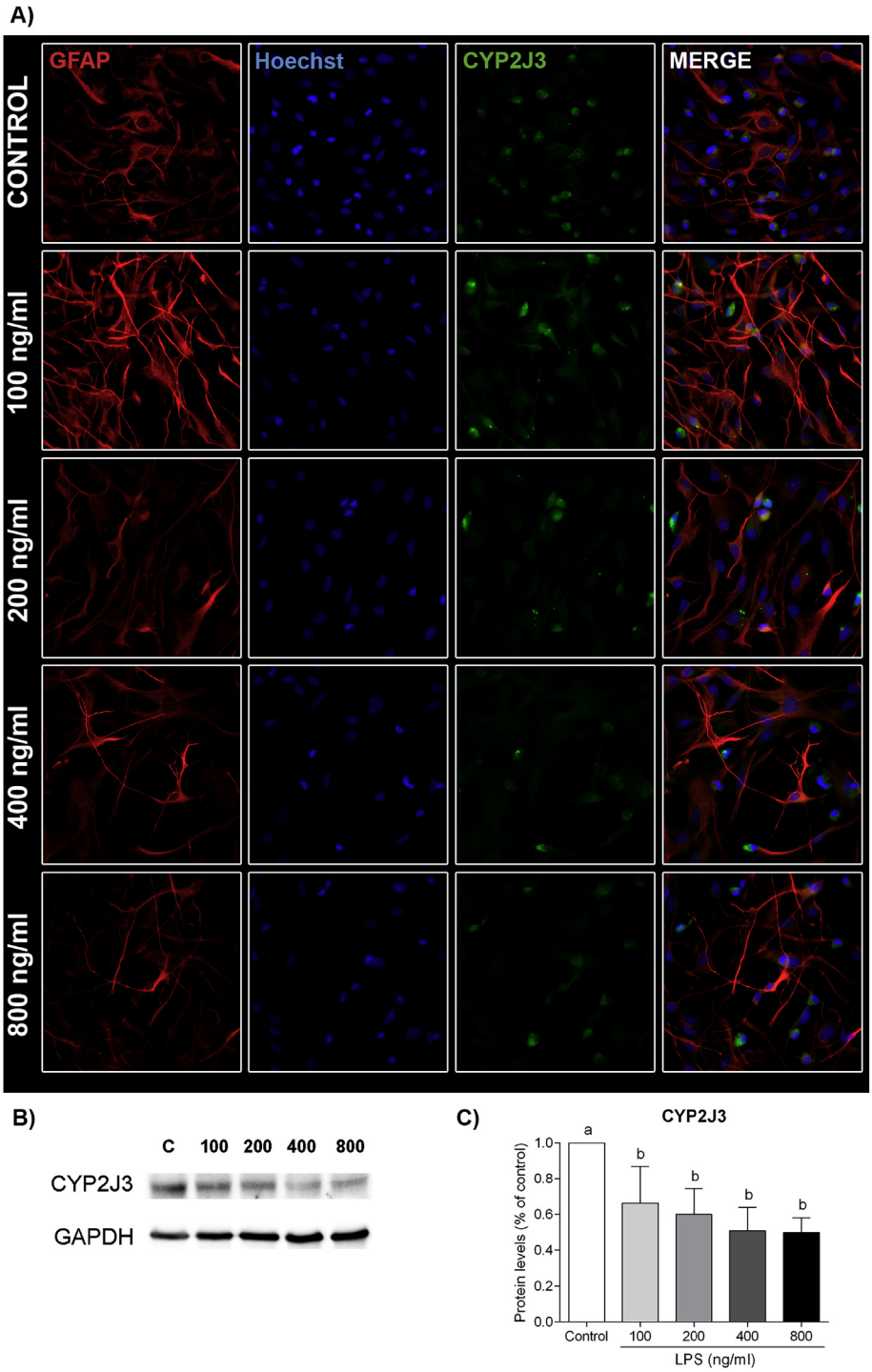

Fig. 2. Effect of LPS treatment in CYP2J3 protein levels in astrocytes. Astrocytes were treated with increasing concentrations of LPS (from 100 to 800 ng/ml) for 24 h. The CYP protein levels were determined by immunofluorescence (A) and by Western Blot (B). Relative quantification of CYP2J3 protein levels was carried out determining band intensities with ImageJ software (C). CYP protein levels were normalized to GAPDH protein levels and the results are shown as the percentage of control (% of control). Three independent experiments were carried out (n = 3). The differences were considered significant when $p < 0.05$. Means with the same letter are not significantly different; means with different letter are significantly different between each other.

1, CYP2C11 4, CYP2J3 1, and CYP2J3 4 oligonucleotides were added to the binding reactions (Fig. 8). The NF-κB consensus commercial labeled oligonucleotide was completely competed by CYP2C11 1 and CYP2C11 4 sequences, as the DNA-protein complexes were almost totally formed by the cold oligonucleotides, observed as no bands (Fig. 8, lanes 4 and 5). Instead, CYP2J3 1 and CYP2J3 2 sequences competed differentially with the consensus sequence, depending on their affinity. CYP2J3 2 showed a greater affinity for NF-κB (Fig. 7B, lane 6); therefore, its cold oligonucleotide competed more and the band disappeared more (Fig. 8, lane 7). CYP2J3 1 also competed with the consensus sequence, but to a lesser extent; therefore, the band of the complexes formed by the consensus oligonucleotide disappeared less (Fig. 8, lane 6).

4. Discussion

In this study, we demonstrate that inflammation is capable of down-regulate the expression, protein levels and activity of CYP epoxygenases in astrocytes and that NF-κB has an important role in this regulation. It has been previously reported that systemic inflammation is able to down-regulate CYP epoxygenases in heart, liver and kidney (Anwar-mohamed et al. 2010). However, in the brain, there is no evidence regarding the regulation of CYP2C and 2J subfamilies (the enzymes with the highest epoxygenase activity). In this work, we studied the regulation of CYP2J3 and CYP2C11 during an inflammatory process in astrocytes. To accomplish this, primary cultures of rat astrocytes were

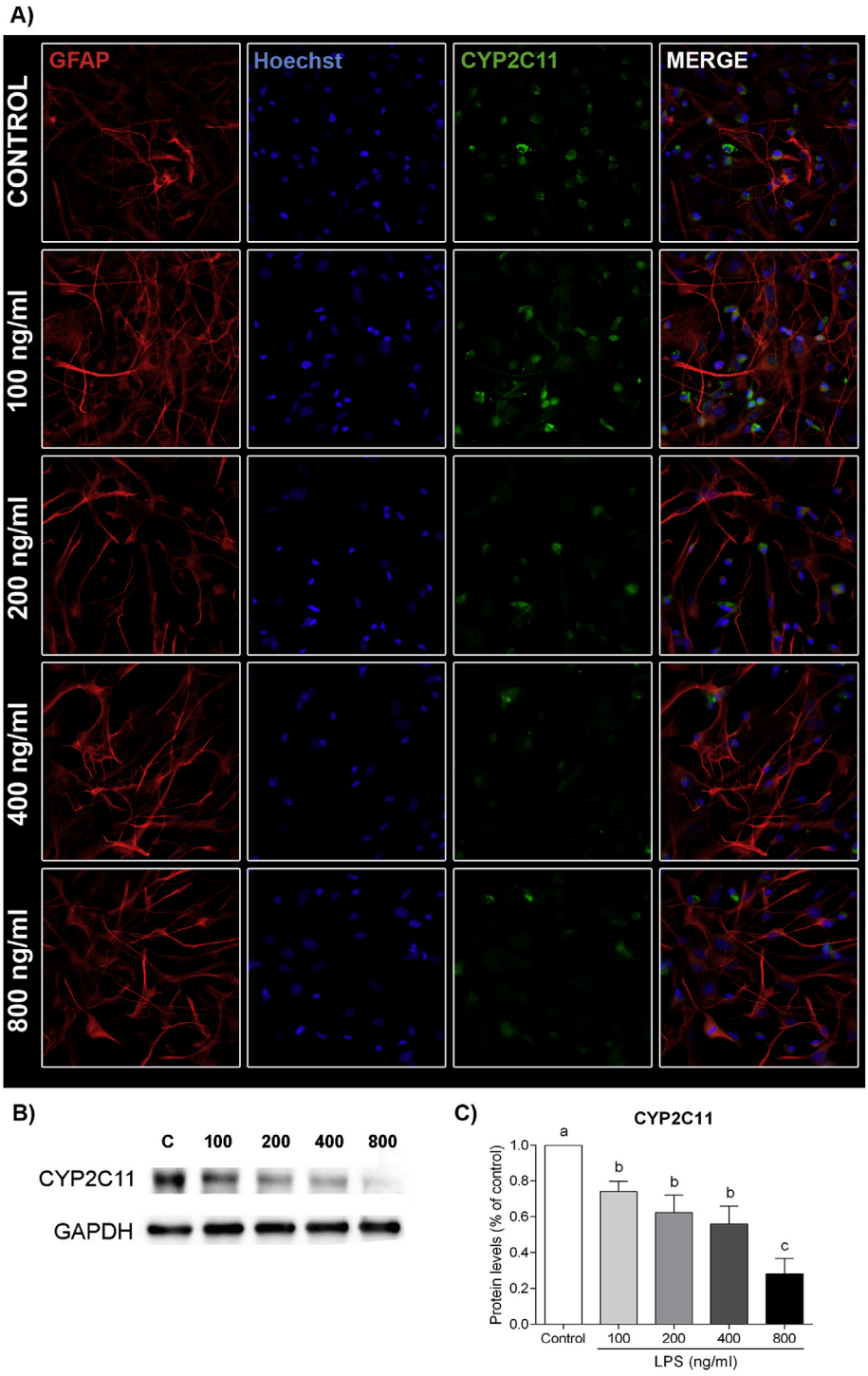

Fig. 3. Effect of LPS treatment in CYP2C11 protein levels in astrocytes. Astrocytes were treated with increasing concentrations of LPS (from 100 to 800 ng/ml) for 24 h. The CYP protein levels were determined by immunofluorescence (A) and by Western Blot (B). Relative quantification of CYP2C11 protein levels was carried out determining band intensities with ImageJ software (C). CYP protein levels were normalized to GAPDH protein levels and the results are shown as the percentage of control (% of control). Three independent experiments were carried out (n = 3). The differences were considered significant when $p < 0.05$. Means with the same letter are not significantly different; means with different letter are significantly different between each other.

stimulated with LPS. The resulting inflammation was able to down-regulate *Cyp2j3* and *Cyp2c11* expression by more than 50% (Fig. 1). *Cyp2c11* was more susceptible to down-regulation, depending on the exposure time, as has been previously observed in other tissues during systemic inflammation (Anwar-mohamed et al. 2010). Otherwise, *Cyp2j3* exhibited an initial decrease in its mRNA levels, which was maintained regardless of the exposure time. It has been previously reported that *Cyp2j3* expression is regulated differentially by inflammation in the heart, kidney, and liver, and is down-regulated in a time-dependent manner only in the liver (Anwar-mohamed et al. 2010).

It had already been reported that *Cyp2c11* is down-regulated in liver or primary rat hepatocytes during inflammation (Wright and Morgan, 1990), mainly as a result of the presence of pro-inflammatory cytokines like IL-1, IL-6, or TNF-α (Chen et al. 1995; Sewer and Morgan, 1997). Cytokine-dependent down-regulation was then attributed to the activation of NF-κB and its binding to a response element within the transcription start site of *Cyp2c11* (Iber et al. 2000). We searched for NF-κB response elements within 4500 base pairs upstream of the ATG start site of *Cyp2c11* and *Cyp2j3* (Fig. 6). Four different putative binding sites were found for each gene, and it was demonstrated that NF-κB is able to bind specifically to them (Fig. 7). This is the first time that the presence of NF-κB specific binding sites is reported within the promoter of *Cyp2j3*, although other mechanisms of transcriptional regulation have already been described (Murray, 2016). However, the most

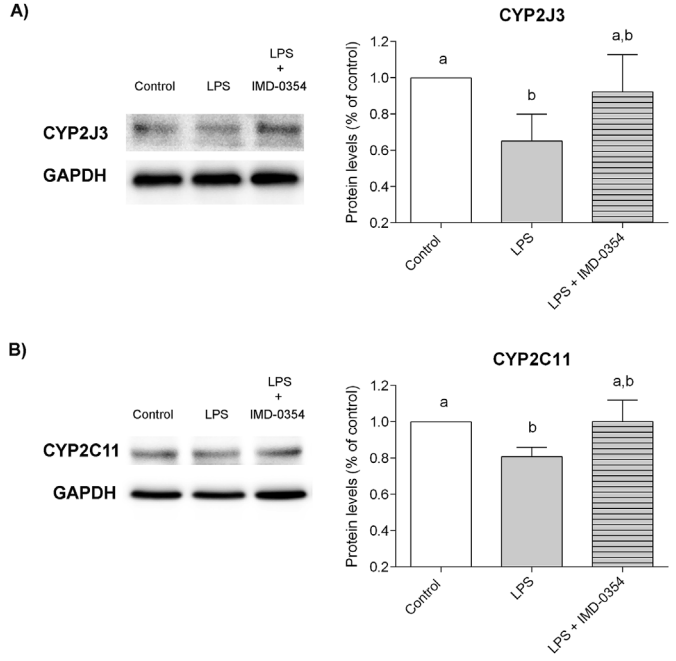

Fig. 4. Effect of NF-κB selective inhibitor (IMD-0354) in CYP2J3 and CYP2C11 protein levels down-regulation. Astrocytes were treated with LPS or LPS + IMD-0354 for 24 h. The CYP2J3 (A) and CYP2C11 (B) protein levels were determined by Western Blot. CYP protein levels were normalized to GAPDH protein levels and the results are shown as the percentage of control (% of control). Three independent experiments were carried out (n = 3). The differences were considered significant when $p < 0.05$. Means with the same letter are not significantly different; means with different letter are significantly different between each other.

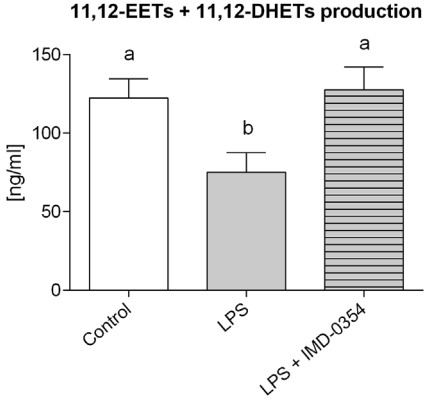

Fig. 5. Total epoxygenase activity determined as the production of 11,12-EET + 11,12-DHET. 11,12-EET and its hydrolyzed product, 11,12-DHET, were measured from the cultured astrocytes stimulated or not with LPS and LPS + IMD-0354 (selective NF-κB inhibitor) using a commercial ELISA kit. Total epoxygenase activity from three independent experiments was measured (n = 3). The differences were considered significant when $p < 0.05$. Means with the same letter are not significantly different; means with different letter are significantly different between each other.

compelling evidence of transcriptional regulation of CYP epoxygenases by NF-κB is the fact that, when the NF-κB pathway was blocked with IMD-0354, the effect of inflammation on *Cyp2j3* and *Cyp2c1*1 mRNA levels was diminished, and was observed as significantly increased mRNA levels for both genes (Fig. 1A and B). It is noteworthy that *Cyp2j3* expression reached control levels (at 12 h) when NF-κB was inhibited, demonstrating that, at least during inflammatory processes, NF-κB is a major player in *Cyp2j3* regulation. Otherwise, even when we found that the *Cyp2c11* promoter region contains at least two NF-κB response elements that bind NF-κB complexes with great affinity (Fig. 7B), the inhibition of NF-κB only partially prevented *Cyp2c11* down-regulation, suggesting that there are additional regulatory mechanisms involved in *Cyp2c11* regulation during inflammation. It had been reported that *Cyp2c11* can be down-regulated by PPAR-α agonists, demonstrating the involvement of PPAR-α in *Cyp2c11* regulation (Corton et al. 1998; Shaban et al. 2005; Večeřa et al. 2011). Additionally, it has also been demonstrated that *Cyp2c11* can be down-regulated via AhR transcription factor and that it could exist a synergistic inhibitory effect with PPAR-α (Shaban et al. 2005).

In addition, CYP2J3 and CYP2C11 protein levels were also decreased by LPS-induced inflammation and this effect was partially prevented when NF-κB pathway was blocked. CYP2C11 protein levels decreased in a LPS dose-response manner (Fig. 3), while CYP2J3 protein levels decreased significantly, but only showed a dose-response tendency (Fig. 2). These results are in accordance with what we observed transcriptionally at 24 h, given that *Cyp2j3* mRNA initially decreased by approximately 60%, but did not decrease further over time (Fig. 1A). When IMD-0354 was concurrently added to LPS, both CYP2J3 and CYP2C11 protein levels were increased ($p < 0.05$; Fig. 4), demonstrating the involvement of NF-κB in this regulation. CYP2J3 is apparently regulated by inflammation only to a certain extent, but this extent is almost completely dependent on NF-κB activity, as it can be seen transcriptionally and in its protein levels. Instead, CYP2C11 is regulated greatly by inflammation, but there may be other pathways involved in addition to the NF-κB pathway, like the nuclear receptor PPAR-α (Shaban et al. 2005; Corton et al. 1998) or the transcription factor AhR (Shaban et al. 2005).

We also found that total EET production was significantly decreased by LPS-induced inflammation, and that it reached control levels when NF-κB was inhibited (Fig. 4). This is in accordance with the fact that CYP2C and CYP2J subfamilies are the major contributors to EET production (Capdevila and Falck, 2000). Therefore, a decrease in CYP2C11 and CYP2J3 levels may be greatly reflected in total EET levels. These results confirm that inflammation down-regulates epoxygenases' activity via NF-κB activation in astrocytes. The significant changes that we found in the levels of these metabolites is a solid evidence of a biological response to these processes, even though 11,12-EET + 11,12-DHET determination by ELISA includes the basal amount of DHETs produced by sEH.

It is now well known that CYP enzymes are regulated during inflammation (Zordoky and El-Kadi, 2009; Morgan, 2001; Aitken et al. 2006). However, the significance that this regulation could have in physiological processes that involve CYP-mediated endogenous metabolism has been much overlooked. CYP epoxygenases and EETs have been proposed as important anti-inflammatory therapeutic targets (Liu et al. 2010; Oni-Orisan et al. 2013; Schmelzer et al. 2005). At the same time, it has been demonstrated that systemic inflammation could regulate CYP epoxygenase levels and EET production (Anwar-mohamed et al. 2010). Therefore, it has been proposed that there is a cycle between inflammation and CYP epoxygenase expression/EET production, which promotes the increase of the inflammatory cascade, and that, if it somehow fails, it could promote chronic inflammatory processes (Shahabi et al. 2014). Hence, it is important to study the regulation of CYP epoxygenases in the central nervous system, where chronic inflammatory processes have been related to the etiology of various neurodegenerative diseases (Pimplikar, 2014; Qin et al. 2007; Hong et al. 2016).

5. Conclusions

LPS-induced inflammation in astrocytes is able to down-regulate CYP2J3 and CYP2C11 mRNA expression, protein levels and total epoxygenase activity. This effect may be due in part to the production of pro-inflammatory cytokines and the subsequent activation of the NF-κB pathway, since its inhibition by IMD-0354 prevented the observed

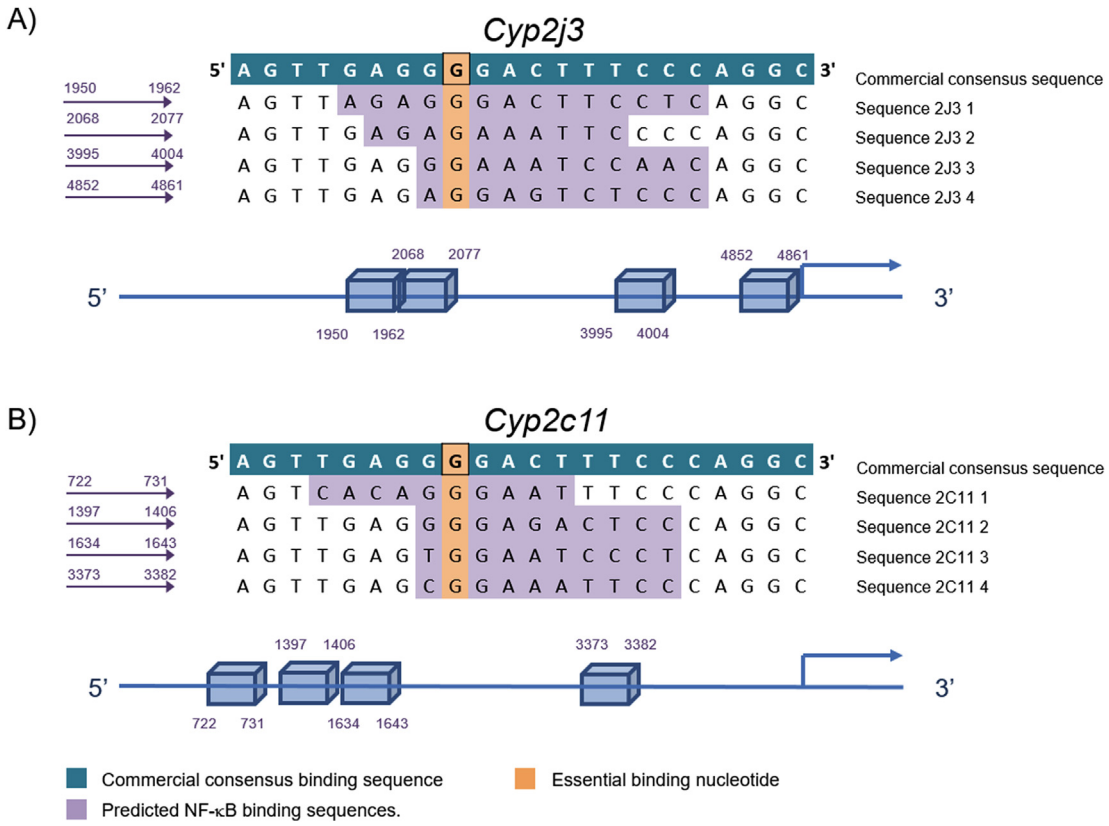

Fig. 6. Putative NF-κB binding site predictions. A search for putative NF-κB binding sites within the *Cyp2j3* (A) and *Cyp2c11* (B) promoter region was conducted. The search was carried out with AliBaba 2.1 free software (BIOBASE) using 4500 base pair upstream of ATG start site. Four putative NF-κB binding sites were found for each gene. Single stranded oligonucleotides were constructed with 22 bases containing the predicted NF-κB binding sequences and they were tested by EMSAs.

effects. Additionally, NF-κB is able to bind specifically to at least two response elements in the promoter region of *Cyp2j3* and *Cyp2c11*, thus indicating that this could be the mechanism by which NF-κB carries out the regulation of these genes.

Conflict of interest

The authors declare that there are no conflicts of interest.

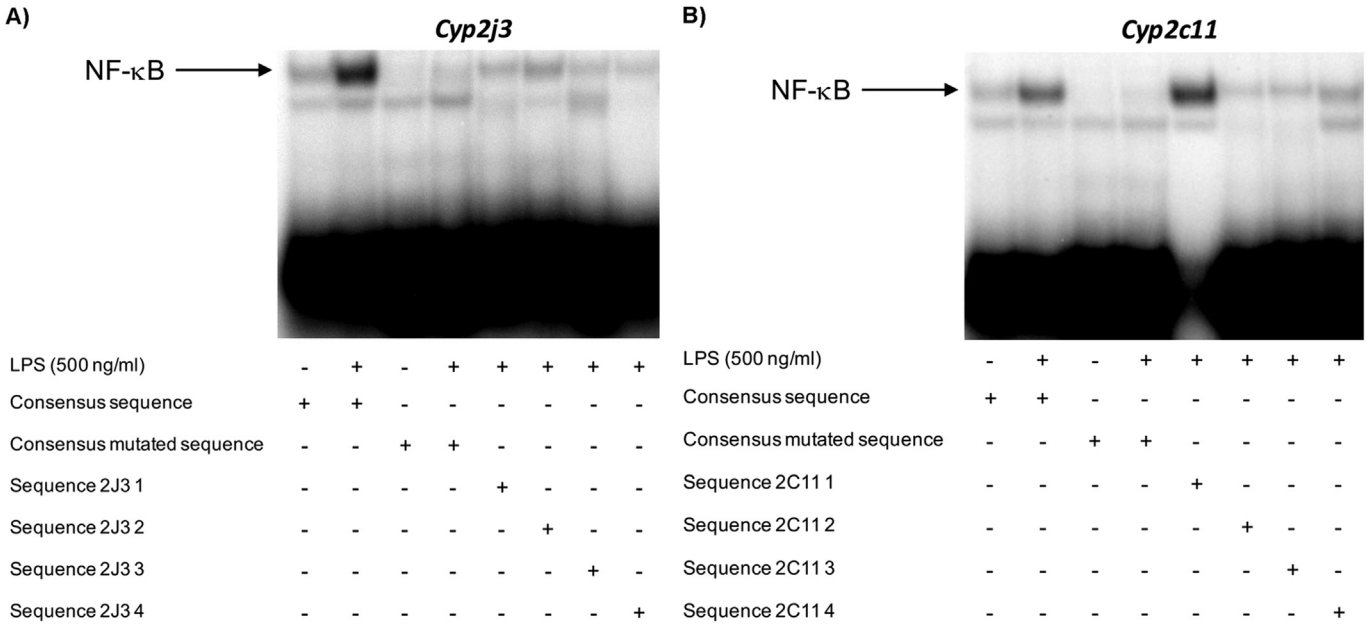

Fig. 7. Electrophoretic Mobility Shift Assays (EMSAs). EMSAs were performed to determine whether NF-κB complexes were able to recognize and bind to the four putative response elements found within *Cyp2j3* (A) and *Cyp2c11* (B) promoter region. 20 μg of the nuclear protein from astrocytes stimulated with 500 ng of LPS for 60 min were incubated with 2 μl of the corresponding γ^{32}-P-labeled oligonucleotide in the binding reactions. NF-κB consensus commercial oligonucleotide was used as positive binding control. NF-κB consensus mutated commercial oligonucleotide was used as negative binding control.

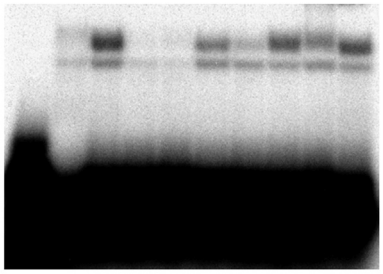

Protein (20 μg)	-	+	+	+	+	+	+	+	+	+
LPS (500 ng/ml)	-	-	+	+	+	+	+	+	+	+
Consensus sequence	+	+	+	+	+	+	+	+	+	+
Cold sequence 2C11 1 (100X)	-	-	-	+	-	-	-	-	-	-
Cold sequence 2C11 4 (100X)	-	-	-	-	+	-	-	-	-	-
Cold sequence 2J3 1 (100X)	-	-	-	-	-	+	-	-	-	-
Cold sequence 2J3 2 (100X)	-	-	-	-	-	-	+	-	-	-
Sequence sox2 (100X)	-	-	-	-	-	-	-	+	-	-
Ab anti-p65 (600 ng)	-	-	-	-	-	-	-	-	+	-
Ab anti-cIAP1 (600 ng)	-	-	-	-	-	-	-	-	-	+

Fig. 8. Supershift and competition controls. Supershift and competition assays were performed to specifically assert the DNA-protein interactions. NF-κB anti-p65 antibody was used to confirm NF-κB identity. As negative control anti-cIAP1 antibody was used. Also, competition assays were performed using cold specific and non-specific oligonucleotides. 100X of cold CYP2C11 1, CYP2C11 4, CYP2J3 1, and CYP2J3 4 oligonucleotides were used to compete with the NF-κB consensus commercial labeled oligonucleotide. As negative control, 100X of sox2 oligonucleotide was used.

Acknowledgments

We would like to thank Sandra Luz Hernández Ojeda for her excellent technical assistance; Tzipe Govezensky for the support in the statistical analysis of this work; Jorge Omar García Rebollar for his technical assistance in the Animal care unit and Miguel Tapia Rodríguez for his technical assistance in the Microscopy unit. Cynthia Navarro-Mabarak was supported by a CONACYT (Consejo Nacional de Ciencia y Tecnología) PhD fellowship No. 356644 to study in the program: Doctorado en Ciencias Biomédicas, Universidad Nacional Autónoma de México.

Appendix A. Supplementary data

Supplementary data to this article can be found online at https://doi.org/10.1016/j.neuint.2019.104499.

References

Abdel-Razzak, Z., Loyer, P., Fautrel, A., Gautier, J.C., Corcos, L., Turlin, B., Beaune, P., Guillouzo, A., 1993. Cytokines down-regulate expression of major cytochrome P-450 enzymes in adult human hepatocytes in primary culture. Mol. Pharmacol. 44, 707–715.

Aitken, A.E., Morgan, E.T., 2007. Gene-specific effects of inflammatory cytokines on cytochrome P450 2C, 2B6 and 3A4 mRNA levels in human hepatocytes. Drug Metab. Dispos. 35, 1687–1693.

Aitken, A.E., Richardson, T.A., Morgan, E.T., 2006. Regulation of drug-metabolizing enzymes and transporters in inflammation. Annu. Rev. Pharmacol. Toxicol. 46, 123–149.

Anwar-mohamed, A., Zordoky, B.N., Aboutabl, M.E., El-Kadi, A.O., 2010. Alteration of cardiac cytochrome P450-mediated arachidonic acid metabolism in response to lipopolysaccharide-induced acute systemic inflammation. Pharmacol. Res. 61, 410–418.

Baldwin, A.S., 1996. The NF-kappa B and I kappa B proteins: new discoveries and insights. Annu. Rev. Immunol. 14, 649–683.

Bell, J.C., Strobel, H.W., 2012. Regulation of cytochrome P450 4F11 by nuclear transcription factor-κB. Drug Metab. Dispos. 40, 205–211.

Blancas-Flores, G., Alarcón-Aguilar, F.J., García-Macedo, R., et al., 2012. Glycine suppresses TNF-α-induced activation of NF-κB in differentiated 3T3-L1 adipocytes. Eur. J. Pharmacol. 689, 270–277.

Capdevila, J.H., Falck, J.R., 2000. Biochemical and molecular characteristics of the cytochrome P450 arachidonic acid monooxygenase. Prostag. Other Lipid Mediat. 62, 271–292.

Carver, K.A., Lourim, D., Tryba, A.K., Harder, D.R., 2014. Rhythmic expression of cytochrome P450 epoxygenases CYP4x1 and CYP2c11 in the rat brain and vasculature. Am. J. Physiol. Cell Physiol. 307, C989–C998.

Chen, J.Q., Ström, A., Gustafsson, J.A., Morgan, E.T., 1995. Suppression of the constitutive expression of cytochrome P-450 2C11 by cytokines and interferons in primary cultures of rat hepatocytes: comparison with induction of acute-phase genes and demonstration that CYP2C11 promoter sequences are involved in the suppressive response to interleukins 1 and 6. Mol. Pharmacol. 47, 940–947.

Corton, J.C., Fan, L.Q., Brown, S., Anderson, S.P., Bocos, C., Cattley, R.C., Mode, A., Gustafsson, J.A., 1998. Down-regulation of cytochrome P450 2C family members and positive acute-phase response gene expression by peroxisome proliferator chemicals. Mol. Pharmacol. 54, 463–473.

Dignam, J.D., Lebovitz, R.M., Roeder, R.G., 1983. Accurate transcription initiation by RNA polymerase II in a soluble extract from isolated mammalian nuclei. Nucleic Acids Res. 11, 1475–1489.

Dutheil, F., Beaune, P., Loriot, M.A., 2008. Xenobiotic metabolizing enzymes in the central nervous system: contribution of cytochrome P450 enzymes in normal and pathological human brain. Biochimie 90, 426–436.

Dutheil, F., Dauchy, S., Diry, M., et al., 2009. Xenobiotic-metabolizing enzymes and transporters in the normal human brain: regional and cellular mapping as a basis for putative roles in cerebral function. Drug Metab. Dispos. 37, 1528–1538.

Fang, X., Hu, S., Watanabe, T., et al., 2005. Activation of peroxisome proliferator-activated receptor alpha by substituted urea-derived soluble epoxide hydrolase inhibitors. J. Pharmacol. Exp. Ther. 314, 260–270.

Fang, X., Hu, S., Xu, B., et al., 2006. 14,15-Dihydroxyeicosatrienoic acid activates peroxisome proliferator-activated receptor-alpha. Am. J. Physiol. Heart Circ. Physiol. 290, H55–H63.

Gu, X., Ke, S., Liu, D., Sheng, T., Thomas, P.E., Rabson, A.B., Gallo, M.A., Xie, W., Tian, Y., 2006. Role of NF-kappaB in regulation of PXR-mediated gene expression: a mechanism for the suppression of cytochrome P-450 3A4 by proinflammatory agents. J. Biol. Chem. 281, 17882–17889.

Hong, H., Kim, B.S., Im, H.I., 2016. Pathophysiological role of neuroinflammation in neurodegenerative diseases and psychiatric disorders. Int. Neurourol. J. 20, S2–S7.

Hung, T.H., Shyue, S.K., Wu, C.H., Chen, C.C., et al., 2017. Deletion or inhibition of soluble epoxide hydrolase protects against brain damage and reduces microglia-mediated neuroinflammation in traumatic brain injury. Oncotarget 8 (61), 103236–103260. https://doi.org/10.18632/oncotarget.21139.

Iber, H., Chen, Q., Cheng, P.Y., Morgan, E.T., 2000. Suppression of CYP2C11 gene transcription by interleukin-1 mediated by NF-kappaB binding at the transcription start site. Arch. Biochem. Biophys. 377, 187–194.

Inceoglu, B., Jinks, S.L., Ulu, A., et al., 2008. Soluble epoxide hydrolase and epoxyeicosatrienoic acids modulate two distinct analgesic pathways. Proc. Natl. Acad. Sci. U. S. A. 105, 18901–18906.

Kanduri, M., Tobin, G., Aleskog, A., Nilsson, K., Rosenquist, R., 2011. The novel NF-κB inhibitor IMD-0354 induces apoptosis in chronic lymphocytic leukemia. Blood Canc. J. 1, e12.

Ke, S., Rabson, A.B., Germino, J.F., Gallo, M.A., Tian, Y., 2001. Mechanism of suppression of cytochrome P-450 1A1 expression by tumor necrosis factor-alpha and lipopolysaccharide. J. Biol. Chem. 276, 39638–39644.

Kelicen, P., Tindberg, N., 2004. Lipopolysaccharide induces CYP2E1 in astrocytes through MAP kinase kinase-3 and C/EBPbeta and -delta. J. Biol. Chem. 279, 15734–15742.

Koerner, I.P., Zhang, W., Cheng, J., Parker, S., Hurn, P.D., Alkayed, N.J., 2008. Soluble epoxide hydrolase: regulation by estrogen and role in the inflammatory response to cerebral ischemia. Front. Biosci. 13, 2833–2841.

Lakkappa, N., Krishnamurthy, P.T., Hammock, B.D., Velmurugan, D., Bharath, M.M., 2016. Possible role of Epoxyeicosatrienoic acid in prevention of oxidative stress mediated neuroinflammation in Parkinson disorders. Med. Hypotheses 93, 161–165.

Lakkappa, N., Krishnamurthy, P.T., P, M.D., Hammock, B.D., Hwang, S.H., 2019. Soluble epoxide hydrolase inhibitor, APAU, protects dopaminergic neurons against rotenone induced neurotoxicity: implications for Parkinson's disease. Neurotoxicology 70, 135–145.

Lakkappa, N., Krishnamurthy, P.T., Yamjala, K., Hwang, S.H., Hammock, B.D., Babu, B., 2018. Evaluation of antiparkinson activity of PTUPB by measuring dopamine and its metabolites in Drosophila melanogaster: LC-MS/MS method development. J. Pharm. Biomed. Anal. 149, 457–464.

Lange, S.C., Bak, L.K., Waagepetersen, H.S., Schousboe, A., Norenberg, M.D., 2012. Primary cultures of astrocytes: their value in understanding astrocytes in health and disease. Neurochem. Res. 37, 2569–2588.

Li, Y., Wu, J., Yu, X., Na, S., Li, K., Yang, Z., Xie, X., Yang, J., Yue, J., 2018. The protective role of brain CYP2J in Parkinson's disease models. Oxid. Med. Cell. Longev. 2018, 2917981.

Liu, J.Y., Yang, J., Inceoglu, B., Qiu, H., Ulu, A., Hwang, S.H., Chiamvimonvat, N., Hammock, B.D., 2010. Inhibition of soluble epoxide hydrolase enhances the anti-inflammatory effects of aspirin and 5-lipoxygenase activation protein inhibitor in a murine model. Biochem. Pharmacol. 79, 880–887.

Liu, M., Alkayed, N.J., 2005. Hypoxic preconditioning and tolerance via hypoxia inducible factor (HIF) 1alpha-linked induction of P450 2C11 epoxygenase in astrocytes. J. Cereb. Blood Flow Metab. 25, 939–948.

López-Bojórquez, L.N., Arechavaleta-Velasco, F., Vadillo-Ortega, F., Móntes-Sánchez, D., Ventura-Gallegos, J.L., Zentella-Dehesa, A., 2004. NF-kappaB translocation and endothelial cell activation is potentiated by macrophage-released signals co-secreted with TNF-alpha and IL-1beta. Inflamm. Res. 53, 567–575.

Martínez-Ramírez, I., Del-Castillo-Falconi, V., Mitre-Aguilar, I.B., et al., 2017. SOX2 as a new regulator of HPV16 transcription. Viruses 9.
Minogue, A.M., Barrett, J.P., Lynch, M.A., 2012. LPS-induced release of IL-6 from glia modulates production of IL-1β in a JAK2-dependent manner. J. Neuroinflammation 9, 126.
Moran, J., Patel, A.J., 1989. Stimulation of the N-methyl-D-aspartate receptor promotes the biochemical differentiation of cerebellar granule neurons and not astrocytes. Brain Res. 486, 15–25.
Morgan, E.T., 2001. Regulation of cytochrome p450 by inflammatory mediators: why and how? Drug Metab. Dispos. 29, 207–212.
Morisseau, C., Hammock, B.D., 2013. Impact of soluble epoxide hydrolase and epoxyeicosanoids on human health. Annu. Rev. Pharmacol. Toxicol. 53, 37–58.
Murray, M., 2016. CYP2J2 - regulation, function and polymorphism. Drug Metab. Rev. 48, 351–368.
Navarro-Mabarak, C., Camacho-Carranza, R., Espinosa-Aguirre, J.J., 2018. Cytochrome P450 in the central nervous system as a therapeutic target in neurodegenerative diseases. Drug Metab. Rev. 50, 95–108.
Nicholson, T.E., Renton, K.W., 1999. Modulation of cytochrome P450 by inflammation in astrocytes. Brain Res. 827, 12–18.
Nicholson, T.E., Renton, K.W., 2001. Role of cytokines in the lipopolysaccharide-evoked depression of cytochrome P450 in the brain and liver. Biochem. Pharmacol. 62, 1709–1717.
Nicholson, T.E., Renton, K.W., 2002. The role of cytokines in the depression of CYP1A activity using cultured astrocytes as an in vitro model of inflammation in the central nervous system. Drug Metab. Dispos. 30, 42–46.
Node, K., Huo, Y., Ruan, X., Yang, B., Spiecker, M., Ley, K., Zeldin, D.C., Liao, J.K., 1999. Anti-inflammatory properties of cytochrome P450 epoxygenase-derived eicosanoids. Science 285, 1276–1279.
Ogawa, H., Azuma, M., Muto, S., et al., 2011. IκB kinase β inhibitor IMD-0354 suppresses airway remodelling in a Dermatophagoides pteronyssinus-sensitized mouse model of chronic asthma. Clin. Exp. Allergy 41, 104–115.
Onai, Y., Suzuki, J., Kakuta, T., Maejima, Y., Haraguchi, G., Fukasawa, H., Muto, S., Itai, A., Isobe, M., 2004. Inhibition of IkappaB phosphorylation in cardiomyocytes attenuates myocardial ischemia/reperfusion injury. Cardiovasc. Res. 63, 51–59.
Oni-Orisan, A., Deng, Y., Schuck, R.N., et al., 2013. Dual modulation of cyclooxygenase and CYP epoxygenase metabolism and acute vascular inflammation in mice. Prostag. Other Lipid Mediat. 104–105, 67–73.
Pimplikar, S.W., 2014. Neuroinflammation in Alzheimer's disease: from pathogenesis to a therapeutic target. J. Clin. Immunol. 34 (Suppl. 1), S64–S69.
Qin, L., Wu, X., Block, M.L., Liu, Y., Breese, G.R., Hong, J.S., Knapp, D.J., Crews, F.T., 2007. Systemic LPS causes chronic neuroinflammation and progressive neurodegeneration. Glia 55, 453–462.
Rawal, S., Morisseau, C., Hammock, B.D., Shivachar, A.C., 2009. Differential subcellular distribution and colocalization of the microsomal and soluble epoxide hydrolases in cultured neonatal rat brain cortical astrocytes. J. Neurosci. Res. 87, 218–227.
Ruparel, S., Henry, M.A., Akopian, A., Patil, M., Zeldin, D.C., Roman, L., Hargreaves, K.M., 2012. Plasticity of cytochrome P450 isozyme expression in rat trigeminal ganglia neurons during inflammation. Pain 153, 2031–2039.
Sarkar, P., Zaja, I., Bienengraeber, M., Rarick, K.R., Terashvili, M., Canfield, S., Falck, J.R., Harder, D.R., 2014. Epoxyeicosatrienoic acids pretreatment improves amyloid β-induced mitochondrial dysfunction in cultured rat hippocampal astrocytes. Am. J. Physiol. Heart Circ. Physiol. 306, H475–H484.
Schmelzer, K.R., Inceoglu, B., Kubala, L., Kim, I.H., Jinks, S.L., Eiserich, J.P., Hammock, B.D., 2006. Enhancement of antinociception by coadministration of nonsteroidal anti-inflammatory drugs and soluble epoxide hydrolase inhibitors. Proc. Natl. Acad. Sci. U. S. A. 103, 13646–13651.
Schmelzer, K.R., Kubala, L., Newman, J.W., Kim, I.H., Eiserich, J.P., Hammock, B.D., 2005. Soluble epoxide hydrolase is a therapeutic target for acute inflammation. Proc. Natl. Acad. Sci. U. S. A. 102, 9772–9777.
Schütze, S., Wiegmann, K., Machleidt, T., Krönke, M., 1995. TNF-induced activation of NF-kappa B. Immunobiology 193, 193–203.
Sewer, M.B., Morgan, E.T., 1997. Nitric oxide-independent suppression of P450 2C11 expression by interleukin-1beta and endotoxin in primary rat hepatocytes. Biochem. Pharmacol. 54, 729–737.
Shaban, Z., Soliman, M., El-Shazly, S., et al., 2005. AhR and PPARalpha: antagonistic effects on CYP2B and CYP3A, and additive inhibitory effects on CYP2C11. Xenobiotica 35, 51–68.
Shahabi, P., Siest, G., Visvikis-siest, S., 2014. Influence of inflammation on cardiovascular protective effects of cytochrome P450 epoxygenase-derived epoxyeicosatrienoic acids. Drug Metab. Rev. 46, 33–56.
Spector, A.A., Norris, A.W., 2007. Action of epoxyeicosatrienoic acids on cellular function. Am. J. Physiol. Cell Physiol. 292, C996–C1012.
Stables, M.J., Gilroy, D.W., 2011. Old and new generation lipid mediators in acute inflammation and resolution. Prog. Lipid Res. 50, 35–51.
Sugita, A., Ogawa, H., Azuma, M., et al., 2009. Antiallergic and anti-inflammatory effects of a novel I kappaB kinase beta inhibitor, IMD-0354, in a mouse model of allergic inflammation. Int. Arch. Allergy Immunol. 148, 186–198.
Tindberg, N., Baldwin, H.A., Cross, A.J., Ingelman-Sundberg, M., 1996. Induction of cytochrome P450 2E1 expression in rat and gerbil astrocytes by inflammatory factors and ischemic injury. Mol. Pharmacol. 50, 1065–1072.
Večeřa, R., Zachařová, A., Orolin, J., Strojil, J., Skottová, N., Anzenbacher, P., 2011. Fenofibrate-induced decrease of expression of CYP2C11 and CYP2C6 in rat. Biopharm Drug Dispos. 32, 482–487.
Wang, L., Luo, G., Zhang, L.F., Geng, H.X., 2018. Neuroprotective effects of epoxyeicosatrienoic acids. Prostag. Other Lipid Mediat. 138, 9–14.
Wright, K., Morgan, E.T., 1990. Transcriptional and post-transcriptional suppression of P450IIC11 and P450IIC12 by inflammation. FEBS Lett. 271, 59–61.
Wu, H.F., Yen, H.J., Huang, C.C., Lee, Y.C., Wu, S.Z., Lee, T.S., Lin, H.C., 2015. Soluble epoxide hydrolase inhibitor enhances synaptic neurotransmission and plasticity in mouse prefrontal cortex. J. Biomed. Sci. 22, 94.
Zhang, W., Koerner, I.P., Noppens, R., et al., 2007. Soluble epoxide hydrolase: a novel therapeutic target in stroke. J. Cereb. Blood Flow Metab. 27, 1931–1940.
Zordoky, B.N., El-Kadi, A.O., 2009. Role of NF-kappaB in the regulation of cytochrome P450 enzymes. Curr. Drug Metabol. 10, 164–178.